Multiple airwaves crossing Britain and Ireland following the eruption of Hunga Tonga–Hunga Ha‘apai on 15 January 2022

Multiple airwaves crossing Britain and Ireland following the eruption of Hunga Tonga–Hunga Ha'apai on 15 January 2022

Stephen Burt
Department of Meteorology, University of Reading, Reading, UK

At 0415 UTC on 15 January 2022, the large subterranean volcano Hunga Tonga–Hunga Ha'apai in the south Pacific Ocean exploded violently, sending an eruption cloud at least 40km into the atmosphere (US Geological Survey, 2022: NASA Earth Observatory, 2022). The volcano is located at 20.546°N, 175.39°W and lies about 68km north–northwest of Nuku'alofa, the capital city of the Kingdom of Tonga. Satellite images caught the dramatic growth of the volcanic plume and the subsequent pressure wave which radiated outward from the volcano at close to the speed of sound. The pressure wave, and its subsequent reverberations, was detected across the entire globe, reaching the British and Irish Isles some 14 hours after the eruption. Its outward ripples are shown nicely in an animation prepared from infrared satellite data which appeared widely in the media in the days following the eruption; Figure 1 shows two frames from this sequence (Barlow, 2022). The resemblance to the airwave patterns deduced by the Royal Society committee following the eruption of Krakatoa in 1883 (Figure 2, from Symons, 1888) – almost 140 years ago, and of course long before modern satellites, digital pressure records and computer models – is pleasingly apparent. The Krakatoa eruption appears to have numerous points in common with Hunga Tonga–Hunga Ha'apai, not least that both were largely instantaneous and extremely violent eruptions of confined and part-submerged volcanic calderas, with resulting great height of atmospheric plumes (Krakatoa's plume reached at least 27–34km; Symons, 1888, pp. 19, 379, 448).

Airwaves in the British and Irish Isles

The British and Irish Isles lie between 16 000 and 17 000km on a great circle route from the site of the eruption (Figure 3). Perhaps contrary to expectation, the shortest great circle route from the eruption site passes close to the North Pole, and thus the 'outbound' wave from the eruption (hereafter, Wave I) crossed the British and Irish Isles almost north to south. Figure 4 shows 1-min detrended pressure observations for the 12-hour period commencing 1600 UTC on 15 January from a selection of sites from north (Lerwick) to south (Jersey), and from Tamanrasset in Algeria very close to the point antipodal to the volcano. The United Kingdom (UK) and Irish sites are located by their initial letter on Figure 5(a). Both the outbound Wave I and its 'rebound' Wave IA are clearly evident on this plot and are discussed further below.

The passage of Wave I

The first 'outbound' Wave I crossed the British and Irish Isles between 1800 and 1900 UTC, as shown on Figure 5(a), which is based upon 1-min resolution digital pressure data from about 40 sites whose positions are indicated. Table 1 lists the characteristics of this first airwave at a selection of these sites. The wave is a pressure-pulse or compression-type wave (longitudinal wave) acting mostly within the denser lower portion of the atmosphere, which is very shallow compared to the radius of the Earth; the form of such waves are discussed in more detail by Gabrielson (2010).

Figure 4 shows that this first wave manifested as a series of rapid rises and falls in pressure over about 30min, followed by an hour or more of very disturbed conditions. The amplitude of the disturbance was sufficient to register on barographs, amounting to a little over 2hPa in many places – slightly greater in the north (2.9hPa at Lerwick), decreasing southwards (1.6hPa in the Channel Islands). Such rapid changes are uncommon, even at major frontal boundaries. The speed of the airwave, calculated from the great circle distance to the site divided by the time elapsed between the eruption and the time of arrival of the airwave at the site, was remarkably consistent, averaging $315 \pm 3 ms^{-1}$ across 35 sites within the British and Irish Isles. There are some minor uncertainties in the calculation, but these do not significantly affect the result: the time of the eruption has been taken from US Geological Survey data, but may have continued for some time and there may have been more than one major blast; the exact time of arrival of the wave is subject to some subjectivity when examining the records; and individual sensor response, lag and averaging times are mostly unknown, although likely to be 1min or less. In all, an uncertainty of even ±5min would lead to an error in wave velocity of only $\pm 2 ms^{-1}$,

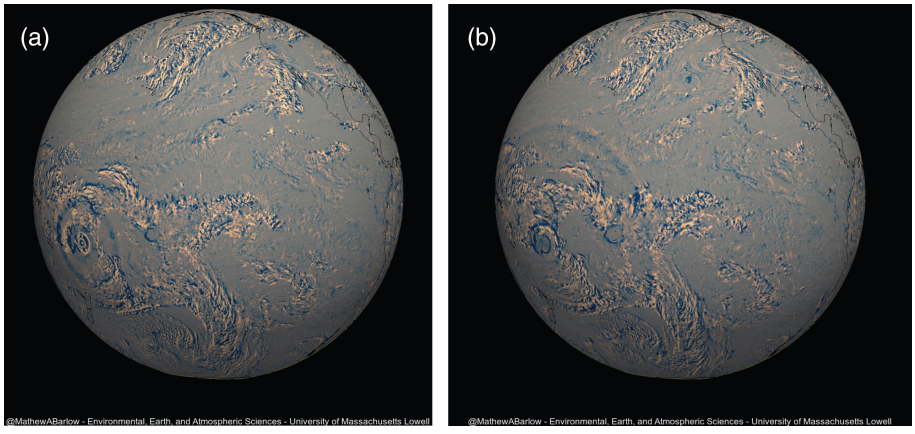

Figure 1. Two frames extracted from an animation prepared by Matthew Barlow of the University of Massachusetts Lowell showing the expanding great circle pressure wave originating at the Hunga Tonga volcano in the south Pacific, prepared from GOES-West infrared satellite data. View the complete animation at https://github.com/mathewbarlow/animations/blob/main/tonga_wave_labeled.gif.

so these results may be taken as reasonably well bounded.

The speed of sound in air at 20°C is 348ms^{-1}. Wave I's derived velocity of 315 ± 3ms^{-1} corresponds to the speed of sound at about −28°C, which is a reasonable approximation to the mid-level temperature of the atmosphere through which the pressure wave passed on its journey from the eruption site.

The wave continued onward past the British and Irish Isles, passing Malaga in the southeast of Spain at 2020 UTC, eventually reaching the eruption's antipodal point (20.55°N, 4.61°E, in the extreme south of Algeria, Figure 3), about 18 hours after the eruption itself. The diameter of the wave as a great circle reached its maximum at 90° from the eruption site and narrowed as it converged upon the antipodal point. As it reached the vicinity of the antipodal point, the wave (now referred to as Wave IA) re-emanated as an expanding circular ripple in the opposite direction, as if from a secondary source at or near that point, from about 2210 UTC. (A second animation showing this 'rebound' can be seen at the reference given in Barlow, 2022.) Particularly interesting is the pressure record from Tamanrasset in southern Algeria (22.8°N, 5.5°E), within a few hundred kilometres of the antipodal point (Figure 3), which shows the arrival of Wave I as a pronounced jump in pressure at 2151 UTC (Figure 4). The speed of the wave upon arrival at Tamanrasset was 310ms^{-1}. The Tamanrasset pressure record suggests that the arrival of the 'inbound' Wave I was followed within 15–20min by two very rapid falls in pressure at the 'departure' of the now diverging outbound Wave IA, amounting in all to a fall of 3.5hPa in 7min from 2213 UTC.

The passage of Wave IA

This 'rebound' Wave IA then retraced the path of the original eruption wave across Europe, south to north this time, detected first at Malaga at 0005 UTC, reaching Jersey at 0057 UTC and departing Shetland 56min later (Figure 5b), eventually converging on the eruption site some 14 hours later after a journey across the globe and back taking just under 36 hours (and averaging about 311ms^{-1} velocity).

The form of Wave IA appeared quite differently to Wave I on pressure records in Britain and Ireland, evident as a series of about 12 well-defined waves with a period of 6–8min, visibly 'cleaner' and more regular than the first disturbance (Figure 4). Each site recorded a rapid fall in pressure in mid-series and a typical overall amplitude of 1.5–1.6hPa. If we take the time of arrival of Wave IA as the time of the first minor peak in the wave train, then we obtain a somewhat greater value for the speed of this return wave: across all 35 sites examined (a

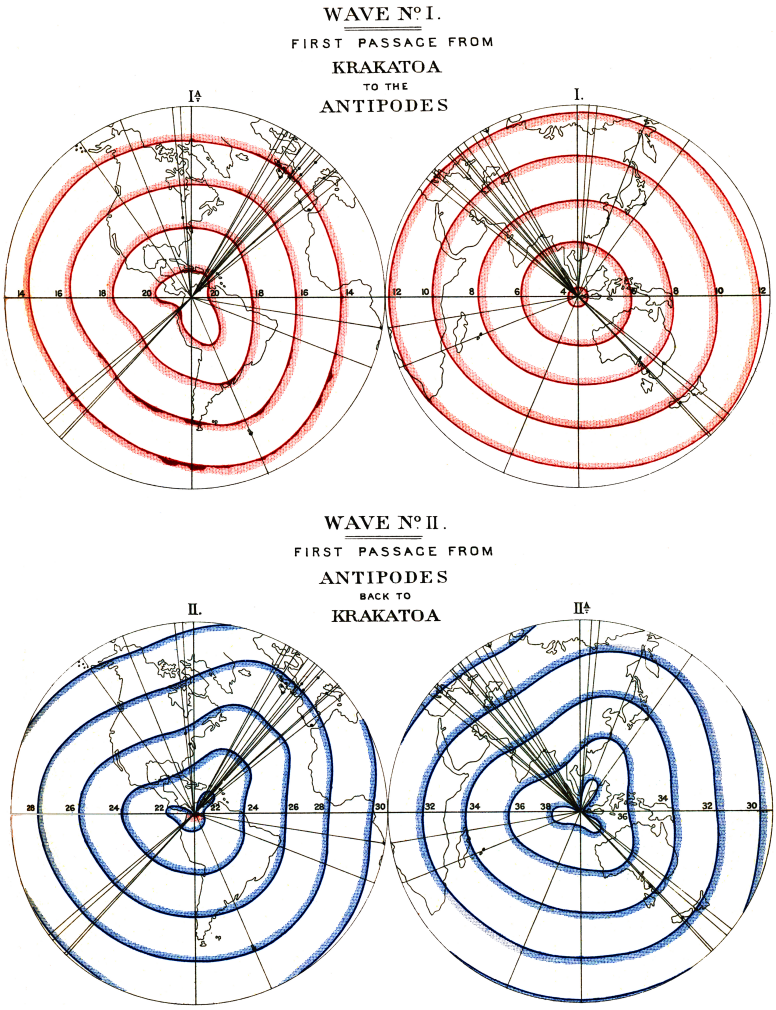

Figure 2. Isochrones at 2-h intervals, to 38 hours, of the first and reflected airwaves following the cataclysmic eruption of Krakatoa (6.1°S, 105.4°W) on 27 August 1883; from Symons, 1888, Plate X.

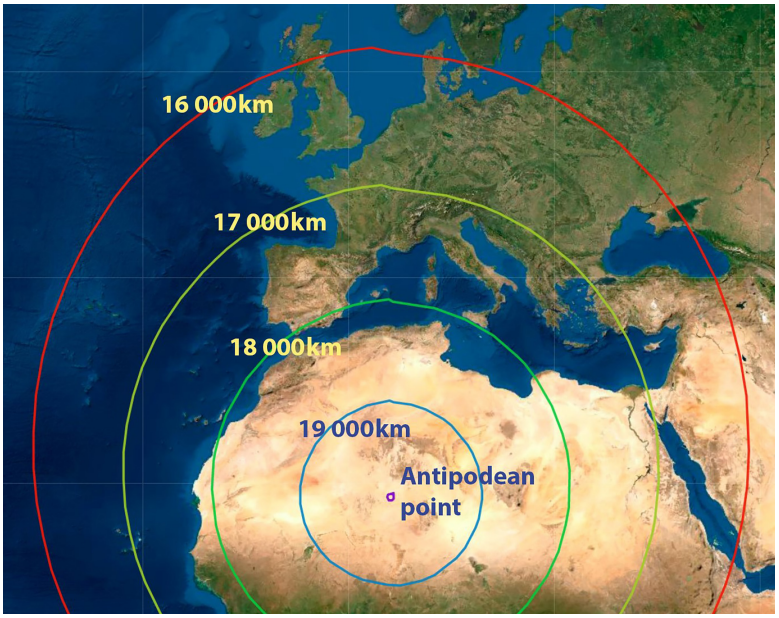

Figure 3. Great circle distances, in kilometres, from the Hunga Tonga–Hunga Ha'apai eruption at 20.55°S, 175.39°W to northwest Europe and north Africa, plotted on a Mercator projection map. The range rings are at 16 000, 17 000, 18 000 and 19 000km; the antipodean point in southern Algeria is indicated at about 20 000km. The 16 000km range ring represents a wave travel time of about 14.1 hours at 315ms^{-1}, and thus the likely position of the wave front at approximately 1820 UTC. Similarly for 17 000km (approximately 1920 UTC), 18 000km (approximately 2010 UTC) and 19 000km (approximately 2105 UTC), while the antipodean point would have been reached about 2200–2205 UTC. Map created at GPSvisualizer.com.

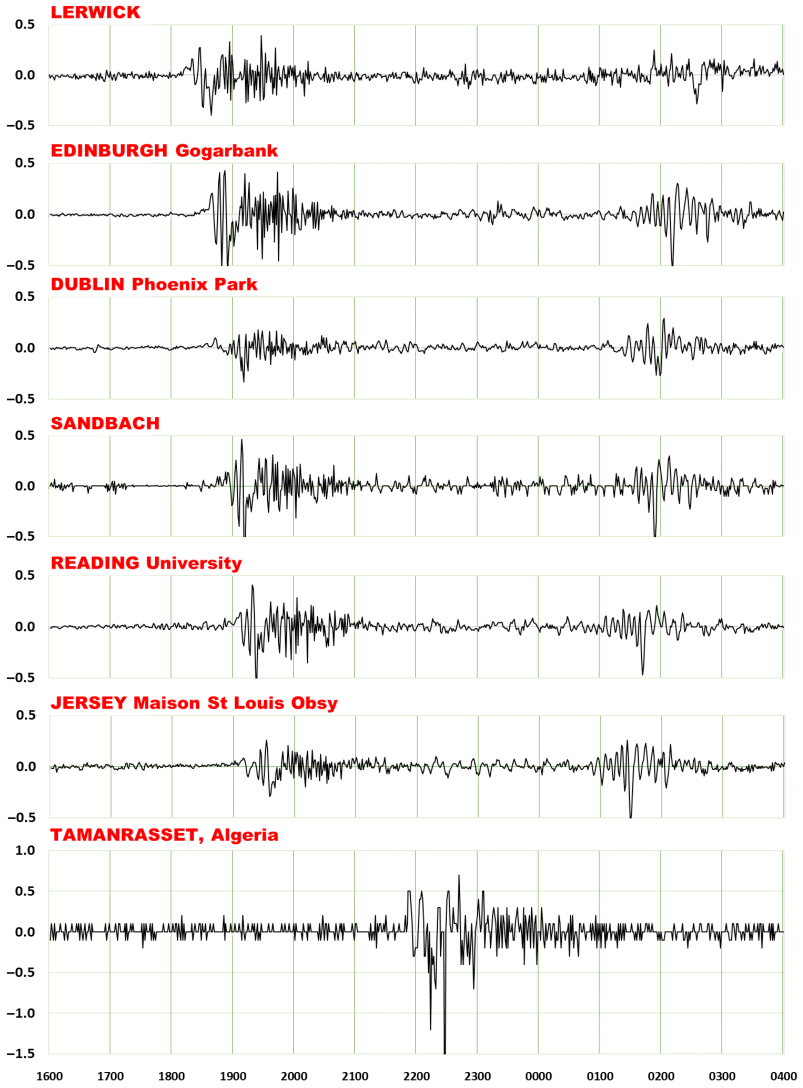

Figure 4. Plotted pressure records from seven sites covering the 12 hours commencing 1600 UTC 15 January 2022, detrended by plotting 1min successive incremental differences. Units in hPa. All of the records shown have data resolution 1min, and all but the Tamanrasset record are from sensors with sensor resolution <0.1hPa. Locations are identified by initial capital letter on Figure 5(a).

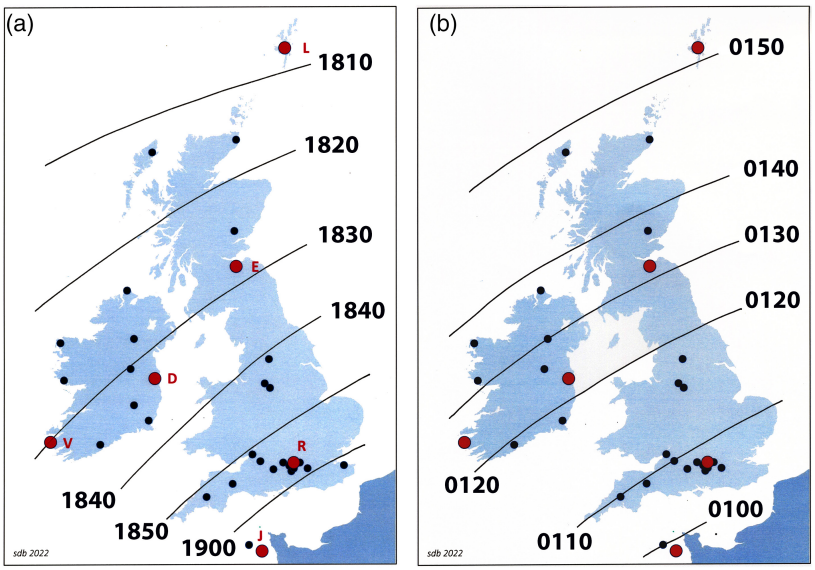

Figure 5. (a) Time of passage in UTC of the 'outward' Wave I across the British and Irish Isles on 15 January 2022. (b) Time of passage in UTC of the 'reflected' Wave IA on 16 January 2022. The red circles show the sites with records plotted on Figure 4 (the initial letter of the site name is shown on (a)); the black circles show additional stations whose records were used to identify arrival times, a selection of which appear in Table 1.

selection of which appear in Table 1), the average is 325 ± 5 ms^{-1}. This corresponds to the speed of sound at −10°C, and it would not be unreasonable to assume a higher mean temperature for Wave IA returning northwards from north Africa than for Wave I passing over the polar regions. If instead the time of arrival is assumed to be coincident with the start of the fall towards the minimum pressure value, then an average wave speed across Britain and Ireland of 275 ± 7 ms^{-1} is obtained, about 13% lower than the 'inbound' Wave I. The truth probably lies somewhere between the two, for the actual wavefront arrival appears obscured within wave superposition and interference patterns between follow-on ripples from Wave I and the oncoming Wave IA. Mid-tropospheric winds were not particularly strong, and broadly from southwest or west and thus almost orthogonal to the passage of both waves, and their effect on the passage of the waves was probably quite minor, although no doubt this and other factors will be evaluated in detailed numerical simulations over the coming months.

Second, third and fourth wave passages

Clear evidence exists of the passage of second, third and fourth waves crossing Britain and Ireland. Figure 6 shows the barometric pressure record from Reading University Atmospheric Observatory for the period 1500 UTC 15 January to 0600 UTC 19 January; similar fluctuations were evident in most other records examined in this analysis. At the Reading Observatory, station-level barometric pressure is logged every second, and the passage of Waves II/IIA and III/IIIA are clearly shown. Waves IV and IVA could also be detected by close analysis of the record (not shown) at around 0530 UTC and 1130 UTC on 20 January, the latter passage 127 hours after the eruption. Thereafter, noise resulting from normal synoptic and diurnal variability make unambiguous identification of the passage of any further waves or reverberations more challenging.

Table 2 shows the time of arrival and amplitude of the various waves at Reading, with derivation of wave speed on each circuit. The amplitude of the waves vary inversely with the logarithm of cumulative distance of the wave from 'eruption zero'.

Have such airwaves occurred previously?

There are numerous documented instances of pressure waves propagating from large atmospheric disturbances, both natural and anthropogenic (conventional explosions and nuclear bomb tests for example), but very few parallel the amplitude of the waves observed on this occasion. The Royal Society's

Table 1

Arrival times of Waves I and IA at a selection of sites within Britain and Ireland, 15/16 January 2022, with derived wave speeds assuming eruption time 0415 UTC 15 January, and antipodal point reached 18 hours later. The sites are arranged in descending order of latitude. Each site location is shown to two decimal places of latitude and longitude in this table, but where available greater precision was used to calculate great circle distances. Each of these sites has 1-min pressure records at a resolution of 0.1hPa or better. The great circle distance for Wave I is from the volcano site (20.55°S, 175.39°W) and for Wave IA from its antipodal point (20.55°N, 4.61°E). Great circle distance calculations are calculated using www.gpsvisualizer.com/calculators. The amplitude (in hPa) is for a period of 60min on either side of the wave arrival time.

			WAVE I – 15 January					WAVE IA – 16 January				
Location	*Latitude °N*	*Longitude °E*	*Arrival time (UTC)*	*Arrival time (min)*	*Gt circle distance (km)*	*Wave speed (ms^{-1})*	*Amplitude (hPa)*	*Arrival time (UTC)*	*Arrival time (min)*	*Gt circle distance (km)*	*Wave speed (ms^{-1})*	*Amplitude (hPa)*
Lerwick Observatory	60.13	−1.18	1807	832	15 585	312.2	2.9	0153	223	4419	330.3	1.2
Wick Airport	58.45	−3.08	1818	843	15 750	311.4	2.5	0147	217	4276	328.4	2.0
Stornoway	58.21	−6.37	1816	841	15 820	313.5	2.5	0147	217	4254	326.7	1.7
Edinburgh, Gogarbank	55.93	−3.35	1829	854	16 021	312.7	2.6	0132	202	3983	328.6	1.7
Belmullet	54.23	−10.01	1821	846	16 238	319.9	1.1	0134	204	3938	321.7	0.8
Bingley	53.82	−1.87	1840	865	16 271	313.5	2.5	0118	188	3734	331.0	1.8
Dublin, Phoenix Park	53.36	−6.35	1834	859	16 162	313.6	1.4	0121	191	3761	328.2	1.7
Mace Head	53.33	−9.90	1825	850	16 338	320.4	1.4	0131	201	3844	318.7	1.2
Smallwood, Sandbach	53.16	−2.33	1843	868	16 337	313.7	2.5	0118	188	3668	325.2	1.8
Newchapel	53.09	−2.21	1843	868	16 346	313.9	2.5	0116	186	3658	327.8	1.8
Valentia Observatory	51.94	−10.20	1830	855	16 487	321.4	1.0	0123	193	3714	320.7	1.3
Roches Point	51.79	−8.24	1832	857	16 523	321.3	1.3	0119	189	3643	321.3	0.8
Almondsbury	51.55	−2.56	1850	875	16 508	314.4	2.1	0111	181	3496	321.9	1.7
Oldland, East Bristol	51.44	−2.48	1849	874	16 522	315.1	2.2	0112	182	3483	319.0	1.9
Reading University	51.44	−0.94	1852	877	16 542	314.4	2.4	0105	175	3462	329.7	1.5
Wokingham	51.42	−0.85	1851	876	16 546	314.8	2.3	0104	174	3459	331.3	1.6
Thatcham	51.41	−1.28	1854	879	16 542	313.7	2.4	0108	178	3463	324.3	1.7
Stratfield Mortimer	51.37	−1.04	1846	871	16 549	316.7	2.3	0106	176	3456	327.3	1.6
Herne Bay	51.37	1.11	1900	885	16 571	312.1	2.4	*No clear arrival signature*				1.4
North Hill, Cornwall	50.56	−4.44	1855	880	16 581	314.0	1.3	0110	180	3424	317.0	1.8
Jersey Observatory	49.10	−2.10	1903	887	16 781	315.3	1.6	0057	167	3223	321.7	1.7

Krakatoa report (Symons, 1888) discussed in detail the significant and multiple airwaves resulting from the main cataclysm at 0256 GMT on 27 August 1883, illustrating the account with miniaturised barograph traces from 40 sites across the world (11 in the British and Irish Isles). The amplitude of the Krakatoa airwaves were summarised by Scott (1883) and amounted to 1.7–2.7hPa – very similar to the present discussion. His paper included scaled reproductions of barograph traces from nine locations in the British Isles. The main Krakatoa report (Symons, 1888) identified and tracked six outbound/rebound waves and part of a seventh (i.e. up to Waves VI/ VIA and VII), up to 126 hours after the main eruption.

The fall and explosion of the Tunguska meteor in Siberia at about 0016 UTC on 30 June 1908 produced a single pronounced airwave across England of amplitude ~0.15hPa (Whipple, 1930; Astapowitsch, 1934; Deacon, 1982), whose velocity was assessed as 290ms^{-1}. This event is particularly interesting because, although barograph jiggles were remarked upon at the time, the cause of the event remained unknown until some 20 years later. The eruption of Mt St Helens in Washington state in the USA at 1532 UTC on 18 May 1980 produced airwaves which were recorded in Europe (sensitive microbarographs in De Bilt and at two sites in Germany), but with barely measurable amplitudes (also ~0.15hPa); the arrival wave speed averaged 308ms^{-1} (Donn and Balachandran, 1981). The largest volcanic eruption in recent decades, that of Mt Pinatubo in the Philippines on 15 June 1991, did generate airwaves which were detected on sensitive infrasound equipment in Japan (Tahira *et al.*, 1996), but it did not result in any significant effects on barograph traces in western Europe: nor did the fall of the Chelyabinsk meteor over the southern Ural region in Russia at about 0320 UTC on 15 February 2013, the largest known natural object to have entered Earth's atmosphere since the Tunguska event. Was the differentiator that Krakatoa and Hunga Tonga–Hunga Ha'apai were both

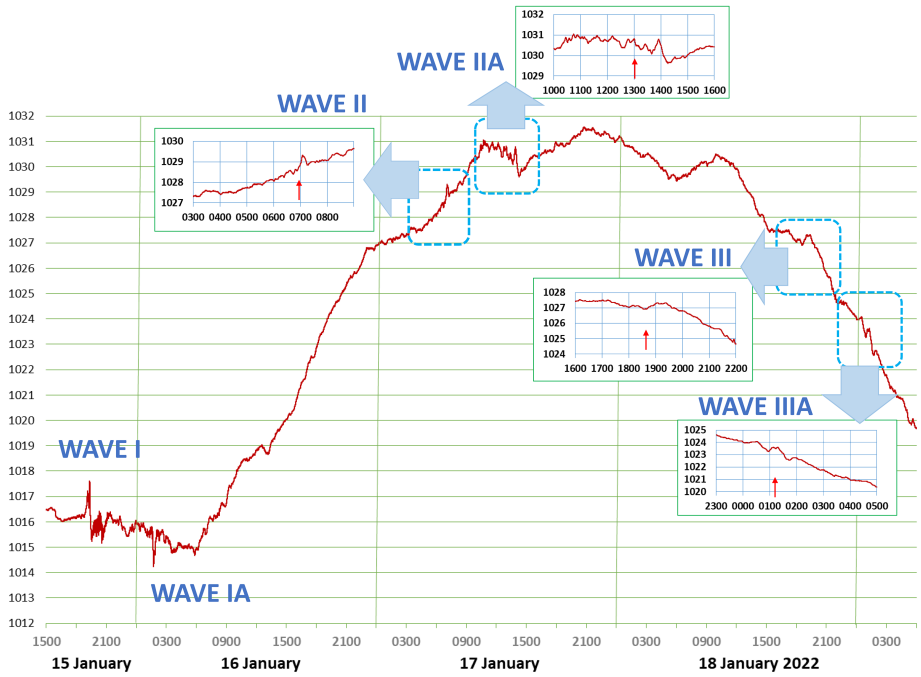

Figure 6. The station-level barometric pressure record, 1s and <0.1-hPa resolution, from the Reading University Atmospheric Observatory for the period 1500 UTC 15 January to 0600 UTC 19 January 2022, identifying the passage of the first three airwaves, with insets showing the pressure record in more detail. Units in hPa. The main plot consists of 313 200 separate data points, and each inset has 21 600 records.

Table 2

Passage times and amplitudes of the airwaves resulting from the Hunga Tonga–Hunga Ha'apai eruption at 0415 UTC on 15 January 2022 observed at the Reading University Atmospheric Observatory (51.441°N, 0.938°W) over the period 15–20 January 2022

	Wave no.							
	I	*IA*	*II*	*IIA*	*III*	*IIIA*	*IV*	*IVA*
Time of arrival (date/time UTC)	15/1852	16/0105	17/0700	17/1300	18/1835	19/0115	20/0530	20/1130
Amplitude (hPa)*	2.38	1.72	1.28	0.87	0.42	0.40	0.26	<0.2
Elapsed time since eruption (h)	14.6	20.8	50.7	56.7	86.3	93.0	121.2	127.2
Segment distance ($m \times 10^6$)	16.5	3.5	40.0	3.5	40.0	3.5	40.0	3.5
Wave velocity over segment (ms^{-1})	315	330	307	321	312	315	318	321
Cumulative distance covered ($m \times 10^6$)	16.5	20.0	60.0	63.5	103.5	107.0	147.0	150.5

*Amplitude taken as the difference between the minimum and maximum barometric pressure within 60min either side of the time of arrival of the wave, although most changes occurred within a shorter period. Synoptic trends distorted wave-related pressure changes from Wave IIIA onwards.

very sudden violent explosions of confined subterranean volcanic calderas, exacerbated by instantaneous contact with enormous volumes of seawater, as opposed to land-based magmatic activity taking place over several hours?

In conclusion, it seems certain that the airwaves resulting from the recent Hunga Tonga–Hunga Ha'apai volcanic eruption were as large as any previously documented in the British and Irish Isles within reliable instrumental records – at least 150 years. The occurrence can thus truly be regarded as a 'once in a lifetime' event.

Acknowledgements

The observations in Table 1 came from both professional and amateur records. Thanks to the UK Met Office and Met Eireann who kindly provided records from their own sites: Met Eireann data (www.met.ie) are published under a Creative Commons Attribution 4.0 International (CC BY 4.0). Members of the Climatological Observers Link (COL) kindly responded *en masse* to my appeal on 17 January for pressure data – unfortunately, too many to thank individually! Many observers sent copies of barograph traces, but most of this analysis required high-precision digital pressure records with accurate timing and 1-min resolution (and a few at 5-min resolution). Giuseppe Petricca (Stornoway) and Jim Galvin (Jersey) kindly provided detailed records from opposite ends of the country. My University of Reading colleagues Ed Hawkins and Liz Stephens drew my attention to the striking Tamanrasset pressure record, which was provided via Sidi Baika (Head of the Tamanrasset regional branch of the Algerian Met Office) and Kiswendsida Guigma (Red Cross Climate Centre).

References

Astapowitsch IS. 1934. Air waves caused by the fall of the meteorite on 30th June, 1908, in Central Siberia. *Q. J. R. Meteorol. Soc.* **60**: 493–504.

Barlow M. 2022. Animations of the initial atmospheric response to the Tonga eruption of 15 January 2022. https://github.com/mathewbarlow/animations. (Accessed 10 February 2022).

Deacon EL. 1982. The 1908 Tunguska explosion. *Weather* **37**: 171–175.

Donn WL, Balachandran NK. 1981. Mount St Helens eruption of 18 May 1980: air waves and explosive yield. *Science* **213**: 539–541.

Gabrielson TB. 2010. Krakatoa and the Royal Society: The Krakatoa explosion of 1883. *Acoustics Today* **6**: 14–19.

NASA Earth Observatory. 2022. Hunga Tonga-Hunga Ha'apai Erupts, https://earthobservatory.nasa.gov/images/149347/hunga-tonga-hunga-haapai-erupts: Dramatic Changes at Hunga Tonga-Hunga Ha'apai. https://earthobservatory.nasa.gov/images/149367/dramatic-changes-at-hunga-tonga-hunga-haapai (accessed 10 February 2022).

Scott RH. 1883. Note on a series of barometrical disturbances which passed over Europe between the 27th and the 31st of August, 1883. *Proc. R. Soc. Lond.* **36**: 139–143.

Symons GJ (ed). 1888. *The Eruption of Krakatoa and Subsequent Phenomena: Report of the Krakatoa Committee of the Royal Society*. Royal Society: London 494 pp.

Tahira M, **Nomura M**, **Sawada Y** ***et al***. 1996. Infrasonic and acoustic-gravity waves generated by the Mount Pinatubo eruption of June 15, 1991, in *Fire and Mud: Eruption and Lahars of Mount Pinatubo, Philippines*. US Geological Survey, pp 601–613. https://pubs.usgs.gov/pinatubo/prelim.html. (accessed 10 February 2022).

US Geological Survey. 2022. M 5.8 Volcanic Eruption - 68 km NNW of Nuku'alofa, Tonga 15 January 2022. https://earthquake.usgs.gov/earthquakes/eventpage/pt22015050/executive (accessed 10 February 2022).

Whipple FJW. 1930. The great Siberian meteor and the waves, seismic and aerial, which it produced. *Q. J. R. Meteorol. Soc.* **56**: 287–304.

Data source

A consolidated dataset of 1-min pressure observations for almost 50 sites from numerous sources used in this paper has been archived as follows:

Dataset Identifier: https://doi.org/10.17864/1947.000359

Creator: Burt, Stephen D.

Title: Pressure_data_Jan_2022 - One-minute resolution barometric pressure data from 46 UK and Irish sites, 15–20 January 2022, assembled to document the atmospheric airwaves emanating from the Hunga Tonga volcanic eruption on 15 January 2022

Publisher: University of Reading

Publication year: 2022

Resource type: Dataset

Version: 1.0

Correspondence to: Stephen Burt

s.d.burt@reading.ac.uk

doi: 10.1002/wea.4182

Spotlight

The first hour of the paroxysmal phase of the 2022 Hunga Tonga–Hunga Ha'apai volcanic eruption as seen by a geostationary meteorological satellite

David Smart

UCL Hazard Centre, University College London, London, UK

The Hunga Tonnga–Hunga Ha'apai islands form part of the rim of a large submarine caldera volcano located some 60–70km north of the island of Tonga in the south-west Pacific ocean. Since December 2014, episodic eruptions at the Hunga volcanic complex have formed new land between two existing islands. The eruptions have largely been of a *Surtseyan* character involving the interaction of hot magma and sea water (Cronin *et al*., 2017). During this time, the volcanic activity has been closely monitored using satellite imagery, including that from instruments aboard polar-orbiter satellites (Garvin *et al*., 2018).

In January 2022, the eruptions entered a new phase with an explosion on 13 January sending an ash plume as high as 12km (CIMSS, 2022a). Soon after 0400 UTC on 15 January (1700h local time) the new island was almost completely destroyed by a catastrophic explosion. The detonation produced a pressure wave that was detected by barometers around the world (see further articles in this issue of *Weather*). Early estimates put the released energy on the order of 10Mt TNT equivalent (NASA, 2022). The ash plume rose to a height of well in excess of 35km (CIMSS, 2022b).

Figure 1 is a sequence of satellite images taken over consecutive 10min periods from 0420 UTC to 0450 UTC on 15 January, showing the evolution of the eruption plume. These images originate from the Himawari-8 geostationary satellite, operated by the Japanese Meteorological Agency (JMA) and were obtained from the Regional and Mesoscale Meteorology Branch (RAMMB) Slider website hosted by the Cooperative Institute for Research in the Atmosphere (CIRA) at Colorado State University.[1] False colour Infrared (IR) imagery is shown in the left-hand column of this figure with the 'proxy-vis' visible channel product in the right column. The actual detonation appears to have occurred just before 0410 UTC (not shown). Both products show the rapid growth of the eruption plume with a concentric ring of cold cloud tops expanding within the first 20min. At 0430 UTC this ring surrounds a central dome of colder cloud tops (with IR temperatures less than −90°C). By 0440 UTC this dome appears to have collapsed with a coincident warming of the central cloud tops. By 0450 UTC further localised cooling of the central area of the plume can be seen with cloud top temperatures below −100°C detected. Imagery from the visible channel product shows shadows being cast northeastwards onto the main 'umbrella' plume, suggesting it is an overshooting top where the buoyant eruption column has risen above the equilibrium level. Preliminary estimates suggest this top reached as high as 55km, well into the stratosphere (CIMSS, 2022b). A more diffuse area of cloud can be seen on the edge of the ash-rich umbrella plume, near the tropopause (height 16–17km), which likely consists of mostly water and ice.

Figure 2 is a snapshot of the plume at 0500 UTC from the Himawari-8 'geo-color' product. At this time, the central part of the plume appears to have collapsed again, suggesting the pulsatile nature of the ascent of the eruption column after the initial explosion. In animated imagery at least one principal pressure wave and a number of smaller ones, evident as a 'brightening' of cloud tops, can be seen propagating away from the eruption epicentre. This is difficult to show in still images but is apparent when an image at one time is subtracted from a previous time, for example at 10min intervals. Using this method, the inferred approximate location, width and direction of motion of this prompt shock wave are indicated in Figure 2. In visible channel

[1]https://rammb-slider.cira.colostate.edu (accessed 20 January 2022).